# Nonclassical characteristic functions for highly sensitive measurements

Th. Richter and W. Vogel

*Arbeitsgruppe Quantenoptik, Fachbereich Physik, Universität Rostock, D-18051 Rostock, Germany*
(Received 29 January 2007; published 29 November 2007)

Characteristic functions are shown to be useful for highly sensitive measurements. Redistributions of motional Fock states of a trapped atom can be directly monitored via the most fragile nonclassical part of the characteristic function. The method can also be used for decoherence measurements in optical quantum-information systems.

## I. INTRODUCTION

The experimental demonstrations of photon antibunching [1], sub-Poissonian photon statistics [2], and quadrature squeezing [3] also led to an increasing interest in practical applications of nonclassical states. An early example is the proposal to use squeezed light for enhancing the sensitivity of interferometric gravitational-wave detection [4]. Experiments have demonstrated the usefulness of squeezed light for improving interferometric measurements [5,6] and spectroscopy [7].

Two decades after the first experimental demonstrations of the potential usefulness of nonclassical states the latter still play a minor role in practical measurements. There may be several reasons for this fact. First, the experimental effort for generating the needed nonclassical states is rather high. Second, some applications, e.g., the use of squeezed light for optimizing the laser power in gravitational-wave detection, can be replaced with developments of laser sources. Third, nonclassical states are usually highly fragile against losses, which may substantially limit their advantages in some applications.

The use of nonclassical states is frequently considered in the context of the reduction of the quantum noise in a certain observable below an ultimate classical noise limit. Examples are the use of sub-Poissonian and squeezed light fields for reducing the noise in direct and homodyne photodetection, respectively. This requires one to link the measurement principle with the observable whose quantum noise is reduced. Below we will reconsider the application of nonclassical states from a much broader point of view. When speaking about nonclassical states in the following, we will only consider quantum states of a single-mode harmonic oscillator whose Glauber-Sudarshan $P$ function is not a probability density [8].

The nonclassicality of quantum states can be completely characterized in terms of measurable characteristic functions of phase-dependent quadratures,

$$\hat{x}_\varphi = \hat{a}e^{i\varphi} + \hat{a}^\dagger e^{-i\varphi}, \tag{1}$$

$\hat{a}$ ($\hat{a}^\dagger$) being the bosonic annihilation (creation) operator and $\varphi$ the phase parameter. To be more specific, a hierarchy of necessary and sufficient conditions has been derived that completely characterizes the nonclassicality of a given quantum state in terms of the quadrature characteristic function $G(k,\varphi)$ [9]. A broad class of nonclassical states can be well

characterized by the rather simple condition of first-order nonclassicality,

$$|G(k,\varphi)| \geq G_{\mathrm{gr}}(k), \tag{2}$$

stating that the absolute value of the characteristic function exceeds, for some arguments, the corresponding value of the ground (or vacuum) state [10].

The signatures of first-order nonclassicality are more general than the quantum-noise reduction of a chosen observable below some classical limit. The condition also includes features such as quantum interference [11] and sub-Planck structures in phase space [12]. Note that the nonclassical effects of first and second order have been experimentally demonstrated for radiation fields [13,14]. The needed characteristic functions can also be observed for the quantized center-of-mass motion of a trapped ion [15,16].

In this paper we propose a measurement principle, where the quadrature characteristic function serves as a highly sensitive probe. It makes use of the fact that the nonclassical signatures of the quadrature characteristic function are more fragile with respect to dissipation than other nonclassical effects, such as sub-Poissonian statistics and squeezing. This provides a tool for the highly sensitive diagnostics of decoherence effects, which is of great interest for quantum information processing.

The paper is organized as follows. In Sec. II we consider the detection of the characteristic function of the quadrature distribution for the motion of trapped ions and for propagating radiation fields. The decoherence is caused in both cases, for example, by a thermal reservoir. Section III is devoted to the use of the most pronounced nonclassical features of the characteristic functions for highly sensitive measurements. A brief summary is given in Sec. IV.

## II. DECOHERENCE IN TERMS OF CHARACTERISTIC FUNCTIONS

Let us consider a nonclassical state $\hat{\rho}(0)$ of a bosonic mode prepared at the initial time $t=0$. Its further evolution is caused by the dissipation to be analyzed, leading to the state $\hat{\rho}(t)$. Eventually, the quadrature characteristic function $G(k,t,\varphi)$ is measured.

In the case of a trapped ion the measurement of $G(k,t,\varphi)$ is performed as follows. An electronic transition is driven simultaneously on the red and the blue motional sidebands in

the resolved sideband regime, which is described by the interaction Hamiltonian [15]

$$\hat{H}_{\text{int}} = \hbar(\Omega\hat{A}_{12} + \Omega^*\hat{A}_{21})\hat{x}_\varphi, \tag{3}$$

where $\hat{A}_{ij} = |i\rangle\langle j|$ $(i,j=1,2)$ is the electronic flip operator and $\Omega$ is the effective Rabi frequency. Most importantly, it is proportional to the quadrature operator $\hat{x}_\varphi$ of the center-of-mass motion, the phase $\varphi$ being controlled by the phase difference of the driving lasers. The total state of the ion is $\hat{\varrho}(t) = \hat{\rho}(t) \otimes \hat{\sigma}(t)$, with a properly prepared electronic state $\hat{\sigma}(t)$. At time $t$ the interaction (3) is switched on for the interaction time $\tau$. The observation of the occupation $\sigma_{11}(t+\tau,\varphi)$ of the electronic ground state directly yields the characteristic function $G(k,t,\varphi)$ of the quadrature distribution [15],

$$G(k,t,\varphi) = 2\left[\sigma_{11}^{(\text{inc})}(t+\tau,\varphi) - \tfrac{1}{2}\right] + 2i\left[\sigma_{11}^{(\text{coh})}(t+\tau,\varphi) - \tfrac{1}{2}\right], \tag{4}$$

where the interaction (3) leads to the scaling $k = 2|\Omega|\tau$. The incoherent and coherent occupations $\sigma_{11}^{(\text{inc})}$ and $\sigma_{11}^{(\text{coh})}$ are measured with the electronic preparations $\sigma_{11}(t)=1$ and $\sigma_{11}(t) = |\sigma_{12}(t)| = \tfrac{1}{2}$, respectively. The electronic-state occupations in Eq. (4) are detected with almost perfect efficiency, by testing (at time $t+\tau$) a transition from the state $|1\rangle$ to an auxiliary state for the appearance of fluorescence [16].

For a radiation field the characteristic function can be sampled in balanced homodyne detection [13,14],

$$G(k,t,\varphi) \approx \frac{1}{N_\varphi}\sum_{j=1}^{N_\varphi} e^{ikx_{\varphi,j}(t)}. \tag{5}$$

Here $x_{\varphi,j}(t)$, $j=1,\ldots,N_\varphi$, is the set of data recorded in balanced homodyning for each setting of $\varphi$. The quadratures describe now the radiation mode at the time $t$. Thus they carry the information on the dissipative interaction contained in the radiation state $\hat{\rho}(t)$.

To illustrate the idea, we deal with a simple model of decoherence caused by a thermal bath of mean occupation number $\bar{n}$. The density operator $\hat{\rho}$ in the interaction picture obeys the master equation

$$\frac{d}{dt}\hat{\rho} = \gamma(\bar{n}+1)[2\hat{a}\hat{\rho}\hat{a}^\dagger - \hat{a}^\dagger\hat{a}\hat{\rho} - \hat{\rho}\hat{a}^\dagger\hat{a}]$$
$$+ \gamma\bar{n}[2\hat{a}^\dagger\hat{\rho}\hat{a} - \hat{a}\hat{a}^\dagger\hat{\rho} - \hat{\rho}\hat{a}\hat{a}^\dagger], \tag{6}$$

with $\gamma$ being the damping rate. The resulting equation for the Wigner characteristic function, $\chi(\xi,t) \equiv \text{Tr}\{\hat{\rho}\exp(\xi\hat{a}^\dagger - \xi^*\hat{a})\}$, has the solution [19]

$$\chi(\xi,t) = \exp\{-(\bar{n}+1/2)|\xi|^2[1-\exp(-2\gamma t)]\}$$
$$\times \chi(\xi\exp(-\gamma t),0), \tag{7}$$

where $\chi(\xi,0)$ is the Wigner characteristic function of the initial quantum state. From this result, the observable quadrature characteristic function

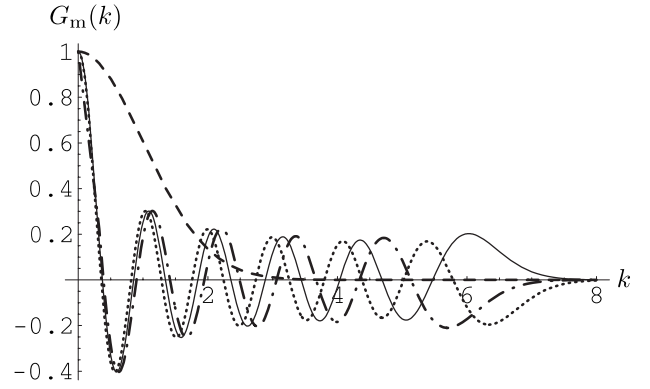$$G(k,t,\varphi) = \chi(ike^{-i\varphi},t) \tag{8}$$

is easily derived.



FIG. 1. Characteristic functions $G_m(k)$ versus $k$ for number states $m=10$ (full line), 9 (dashed-dotted line), and 11 (dotted line), together with the classical limit $G_{\text{gr}}(k) = e^{-k^2/2}$ (dashed line).

## III. HIGHLY SENSITIVE DETECTION

### A. Decoherence of a trapped ion

Let us first consider a trapped atom that is initially in the number state $|m\rangle$, which can be realized in experiments [17]. The motional-state redistributions caused by the reservoir lead to strong modifications of the nonclassical signatures of the characteristic function, which represents our highly sensitive probe. Note that the observed decoherence of a Raman-driven trapped ion [17] is not completely understood yet. Although dephasing mechanisms could be identified [18], a deeper insight in the role of motional states is still required.

The Wigner characteristic function of the number state $|m\rangle$ is given by

$$\chi_m(\xi) = L_m(|\xi|^2)\exp(-|\xi|^2/2), \tag{9}$$

where $L_m(x)$ is a Laguerre polynomial of order $m$. Since the state $|m\rangle$ is phase independent, we may write $G_m(k,\varphi) = G_m(k)$. In Fig. 1 we show the quadrature characteristic functions $G_m(k) \equiv G_m(k,t=0)$ as functions of $k$, for $m = 9,10,11$. Clearly, the first-order nonclassicality condition (2) is fulfilled for all the shown number states. For our examples, the first-order nonclassical effect is most pronounced at the outermost local extremum, where $|G_m(k)| - G_{\text{gr}}(k)$ becomes maximal.

Now we consider the time evolution of the characteristic function $G_m(k,t)$, caused by the thermal reservoir. The initial preparation of a Fock state $|m\rangle$ allows one to distinguish motional-state redistribution effects from dephasing effects. Using Eqs. (7)–(9), we obtain

$$G_m(k,t) = \exp\{-\bar{n}[1-\exp(-2\gamma t)]k^2\}L_m(k^2e^{-2\gamma t})\exp(-k^2/2). \tag{10}$$

This function can be monitored for a chosen time $t$, as discussed in connection with Eq. (4).

To get more insight into the time evolution, we consider the time derivative of the characteristic function at $t=0$,
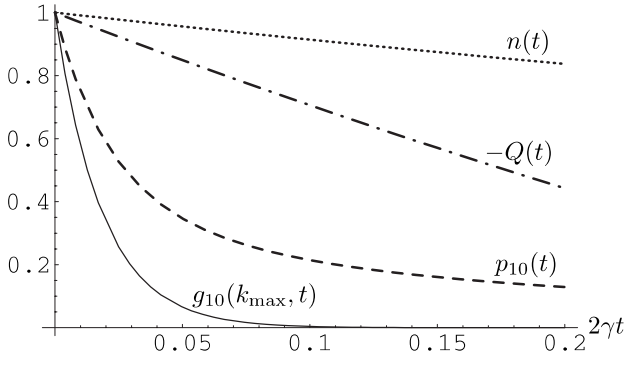
FIG. 2. The time evolution is shown for the occupation probability $p_{10}(t)$ of the state $|m=10\rangle$, the normalized mean excitation number $n(t)$, the Mandel parameter $Q(t)$, and the normalized characteristic function $g_{10}(k_{max},t)$ for $\bar{n}=1$.

$$\dot{G}_m(k,0) = 2\gamma[L_{m-1}^{(1)}(k^2) - \bar{n}L_m(k^2)]k^2 e^{-k^2/2}. \quad (11)$$

It strongly depends on both $k$ and $\bar{n}$; for $m=10$ the maximum of the time derivative occurs for $k=k_{max} \approx 6$. Hence this argument of the characteristic function will be of particular interest to detect the decoherence in a sensitive way. Comparing with Fig. 1, the most sensitive reaction on the motional-state redistributions occurs around the outermost maximum of the initial characteristic function, where the nonclassical features are dominant. This reflects the expected high fragility of nonclassical effects.

For the used Fock state it is interesting to compare the time evolution of the characteristic function with that of the sub-Poissonian statistics. For the Mandel parameter $Q = [\langle(\Delta\hat{n})^2\rangle - \langle\hat{n}\rangle]/\langle\hat{n}\rangle$, which measures the deviation from the Poissonian statistics, we get

$$Q(t) = \frac{(\bar{n}^2 - 2\bar{n}m - m)e^{-4\gamma t} + 2\bar{n}(m-\bar{n})e^{-2\gamma t} + \bar{n}^2}{me^{-2\gamma t} + \bar{n}(1 - e^{-2\gamma t})}. \quad (12)$$

Negative values of $Q$ characterize a nonclassical quantum state showing sub-Poissonian statistics.

In Fig. 2 we show the time evolution of the normalized characteristic function, $g_{10}(k,t) = G_{10}(k,t)/G_{10}(k,0)$, for $k = k_{max}$ and $\bar{n}=1$. For comparison, the time evolutions are also shown for the Mandel $Q$ parameter, the occupation probability $p_{10}(t)$ of the initially prepared Fock state $|m=10\rangle$, and the normalized mean motional-state excitation $n(t)$, $n(t) = \langle\hat{n}(t)\rangle/\langle\hat{n}(0)\rangle$, with $\langle\hat{n}(t)\rangle = me^{-2\gamma t} + \bar{n}(1 - e^{-2\gamma t})$. It is clearly seen that the nonclassical characteristic function shows the fastest decay and evolves much faster than the nonclassical property described by the Mandel $Q$ parameter. In fact, the nonclassical part of the characteristic function decays even faster than the occupation probability of the initially prepared Fock state. Thus it yields a highly sensitive means of detection, since even tiny dissipation leads to a noticeable effect on that part of the characteristic function.

How can we explain the highly sensitive behavior of the characteristic function in its outermost maximum? The quadrature characteristic function,

$$G_{10}(k,t) = \sum_{n=0}^{\infty} p_n(t)G_n(k), \quad (13)$$

can be written as a sum of characteristic functions of number states weighted with the occupation probabilities $p_n(t)$. From the master equation (6) it follows that at the very beginning of the time evolution the only nonvanishing occupation probabilities are $p_9(t)$, $p_{11}(t)$, and $p_{10}(t) = 1 - p_9(t) - p_{11}(t)$. It is seen from Fig. 1 that $G_9(k)$ and $G_{11}(k)$ attain for $k = k_{max}$ roughly the same absolute value as $G_{10}(k)$, but with opposite sign. Thus, according to Eq. (13), the increase of $p_9(t)$ and $p_{11}(t)$ leads to a faster decay of $G_{10}(k,t)$ compared with $p_{10}(t)$. The decay of $G_{10}(k_{max},t)$ is roughly twice as fast as the decay of $p_{10}(t)$. Hence the detection of the characteristic function is both simpler and more sensitive than a number-state measurement, even though the latter is directly related to the prepared number state.

For comparison we may look at the characteristic function for other $k$ values, which are within the classical region (such as $k \approx 1$) or which violate the classical limit only slightly (e.g., $k \approx 2$). Then the temporal evolution is significantly slower. For $k \approx 1$ the neighboring functions are almost equal: $G_9(k) \approx G_{10}(k) \approx G_{11}(k)$, cf. Fig. 1. Thus increasing values of $p_9$ and $p_{11}$ nearly compensate the decay of $p_{10}$, resulting in a slow decay of $G_{10}(k,t)$.

### B. Decoherence of radiation fields

In the following we will consider a typical application of our method that could be realized for a radiation field. The aim is to identify small decoherence effects during the transmission of nonclassical light through media. This is of great importance for applications such as in quantum communication, where the transmission can be performed via optical fibers or through the atmosphere.

The preparation of photon number states, at least for larger photon numbers, is much more difficult to realize as the Fock-state preparation in the ion trap. However, we will see that squeezed light can be used as the nonclassical radiation source for our measurement principle as well. Let us consider a squeezed vacuum,

$$|sv\rangle = \exp[-(r/2)\hat{a}^{\dagger 2} + (r/2)\hat{a}^2]|0\rangle, \quad (14)$$

with $r \geq 0$. The action of the medium is modeled by the thermal reservoir as before.

Due to the contact with the reservoir, the minimum of the quadrature variance [$\varphi = 0$ in Eq. (1)] behaves like

$$\langle[\Delta\hat{x}(t)]^2\rangle_{min} = (1 + 2\bar{n})(1 - e^{-2\gamma t}) + e^{-2r}e^{-2\gamma t}, \quad (15)$$

where $t$ represents the propagation time through the medium. For the chosen phase $\varphi = 0$ the nonclassical effect is most pronounced. The characteristic function for this phase is simply given by

$$G_{sv}(k,t) = e^{-k^2\langle[\Delta\hat{x}(t)]^2\rangle_{min}/2}. \quad (16)$$

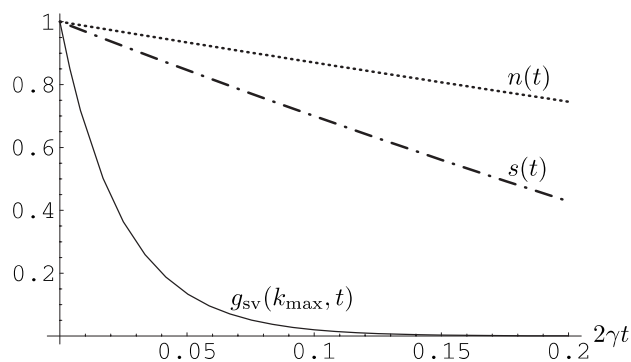Its time derivative yields the $k$ value with the maximum sensitivity of our method to be

FIG. 3. Time evolution of the normalized mean photon number $n(t)$, the quadrature variance $s(t)$, and the characteristic function $g_{sv}(k_{max},t)$ of an initial squeezed vacuum state with $r=1.32$ for $\bar{n}=1$.

$$k_{max} = \sqrt{2e^{2r}}, \tag{17}$$

which is independent of the value of $\bar{n}$.

In Fig. 3 we show the time evolution of the normalized mean photon number $n(t)$, the normally ordered quadrature variance $s(t)$, and the characteristic function $g_{sv}(k,t)$, where

$s(t)=\langle:[\Delta\hat{x}(t)]^2:\rangle_{min}/\langle:[\Delta\hat{x}(0)]^2:\rangle_{min}$ and $g_{sv}(k,t)=G_{sv}(k,t)/G_{sv}(k,0)$. As expected, the fastest decay is observed for the characteristic function at $k=k_{max}$. To detect this highly sensitive reaction on the reservoir effects, the characteristic function can be sampled, at the end of the transmission channel, via balanced homodyne detection. For the sensitive detection method under study, we only need to consider the behavior for $k=k_{max}$ and for the phase with the minimal quadrature variance.

## IV. SUMMARY

In conclusion, we have shown that highly sensitive measurements can be performed by detecting the strongly nonclassical part of the quadrature characteristic function. The method makes use of the high fragility of the nonclassical effects. For example, the direct observation of the characteristic function can monitor the redistribution of the motional-state occupations of an initially prepared Fock state of a trapped ion. Sensitive optical decoherence measurements can be realized by using squeezed light. The method may be useful for highly sensitive noise control in quantum-information systems. It is based on a universal measurement principle, which can be used with different types of initially prepared nonclassical states.

[1] H. J. Kimble, M. Dagenais, and L. Mandel, Phys. Rev. Lett. **39**, 691 (1977).

[2] R. Short and L. Mandel, Phys. Rev. Lett. **51**, 384 (1983).

[3] R. E. Slusher, L. W. Hollberg, B. Yurke, J. C. Mertz, and J. F. Valley, Phys. Rev. Lett. **55**, 2409 (1985).

[4] C. M. Caves, Phys. Rev. D **23**, 1693 (1981); R. Loudon, Phys. Rev. Lett. **47**, 815 (1981).

[5] M. Xiao, L.-A. Wu, and H. J. Kimble, Phys. Rev. Lett. **59**, 278 (1987).

[6] P. Grangier, R. E. Slusher, B. Yurke, and A. La Porta, Phys. Rev. Lett. **59**, 2153 (1987).

[7] E. S. Polzik, J. Carri, and H. J. Kimble, Phys. Rev. Lett. **68**, 3020 (1992).

[8] U.M. Titulaer and R.J. Glauber, Phys. Rev. **140**, B676 (1965); L. Mandel, Phys. Scr. T **12**, 34 (1986).

[9] Th. Richter and W. Vogel, Phys. Rev. Lett. **89**, 283601 (2002).

[10] W. Vogel, Phys. Rev. Lett. **84**, 1849 (2000).

[11] W. Vogel and D.-G. Welsch, *Quantum Optics* (Wiley-VCH, Weinheim, 2006).

[12] W. H. Zurek, Nature (London) **412**, 712 (2001).

[13] A. I. Lvovsky and J. H. Shapiro, Phys. Rev. A **65**, 033830 (2002).

[14] A. Zavatta, V. Parigi, and M. Bellini, Phys. Rev. A **75**, 052106 (2007).

[15] S. Wallentowitz and W. Vogel, Phys. Rev. Lett. **75**, 2932 (1995); Phys. Rev. A **54**, 3322 (1996).

[16] P. C. Haljan, K.-A. Brickman, L. Deslauriers, P. J. Lee, and C. Monroe, Phys. Rev. Lett. **94**, 153602 (2005).

[17] D. M. Meekhof, C. Monroe, B. E. King, W. M. Itano, and D. J. Wineland, Phys. Rev. Lett. **76**, 1796 (1996).

[18] C. Di Fidio and W. Vogel, Phys. Rev. A **62**, 031802(R) (2000).

[19] P. Marian and T. A. Marian, J. Phys. A **33**, 3595 (2000).